

See discussions, stats, and author profiles for this publication at: <https://www.researchgate.net/publication/265093087>

Electrochemical Photodegradation Study of Semiconductor Pigments: Influence of Environmental Parameters

ARTICLE *in* ANALYTICAL CHEMISTRY · AUGUST 2014

Impact Factor: 5.64 · DOI: 10.1021/ac502303z · Source: PubMed

CITATIONS

5

READS

108

6 AUTHORS, INCLUDING:



Willemien Anaf

University of Antwerp

7 PUBLICATIONS 21 CITATIONS

[SEE PROFILE](#)



Stanislav A Trashin

University of Antwerp

33 PUBLICATIONS 255 CITATIONS

[SEE PROFILE](#)



Koen Janssens

University of Antwerp

380 PUBLICATIONS 5,136 CITATIONS

[SEE PROFILE](#)



Karolien De Wael

University of Antwerp

93 PUBLICATIONS 580 CITATIONS

[SEE PROFILE](#)

Electrochemical Photodegradation Study of Semiconductor Pigments: Influence of Environmental Parameters

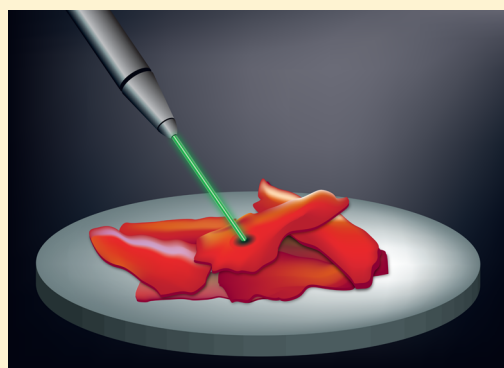
Willemien Anaf,[†] Stanislav Trashin,[†] Olivier Schalm,[‡] Dennis van Dorp,[§] Koen Janssens,[†] and Karolien De Wael^{*,†}

[†]AXES, Department of Chemistry, University of Antwerp, Groenenborgerlaan 171, 2020 Antwerpen, Belgium

[‡]Conservation Studies, University of Antwerp, Blindestraat 9, 2000 Antwerpen, Belgium

[§]IMEC, Kapeldreef 75, 3001 Leuven, Belgium

ABSTRACT: Chemical transformations in paintings often induce discolorations, disturbing the appearance of the image. For an appropriate conservation of such valuable and irreplaceable heritage objects, it is important to have a good know-how on the degradation processes of the (historical) materials: which pigments have been discolored, what are the responsible processes, and which (environmental) conditions have the highest impact on the pigment degradation and should be mitigated. Pigment degradation is already widely studied, either by analyzing historical samples or by accelerated weathering experiments on dummies. However, in historic samples several processes may have taken place, increasing the complexity of the current state, while aging experiments are time-consuming due to the often extended aging period. An alternative method is proposed for a fast monitoring of degradation processes of semiconductor pigments, using an electrochemical setup mimicking the real environment and allowing the identification of harmful environmental parameters for each pigment. Examples are given for the pigments cadmium yellow (CdS) and vermilion (α -HgS).



In the second half of the 19th century, numerous new pigments have been introduced in the painter's palette such as cadmium yellow (CdS), titanium white (TiO₂), or viridian green (Cr₂O₃·2H₂O). In some cases, these "modern" pigments already show remarkable signs of degradation and unstable behavior. An example is cadmium yellow.¹ Characteristic is the fading of the yellow color, probably caused by photoinduced oxidation of cadmium sulfide (CdS) to hydrated cadmium sulfate (CdSO₄·xH₂O), observed in, for example, *Still Life with Coffeepot, Cabbages and Mask* by Ensor.² The presence of other compounds such as cadmium carbonate (CdCO₃) has been established, either originating from the pigment manufacturing process or forming in a secondary reaction between CdSO₄·xH₂O and atmospheric CO₂. This occurred for example in the painting *Le Bonheur de Vivre* by Matisse.³ More complex secondary reactions were observed in *Flowers in a Blue Vase* by Van Gogh, where the degraded CdS paint was covered with a varnish containing lead-based driers and oxalate ions.⁴ Only recently, one starts to understand that the 19th century inorganic pigments are more prone to deterioration than was ever expected. Moreover, only the pigments most sensitive to transformations have been investigated. Such pigments do not show pronounced deterioration yet. Though, to improve the environmental conditions in which the paintings are stored and housed, the prediction of their sensitivity to the most important environmental parameters, well before actual deterioration takes place, is crucial.

On the other hand, pigments that were introduced centuries ago often already show a well-pronounced degradation due to the extended natural aging times. An example is the red pigment α -HgS, used since antiquity. It is called cinnabar in its natural form and vermilion in its synthetic form. Degradation can induce a black discoloration of the initial bright red pigment, which was recently related to the formation of metallic mercury.⁵ Examples are the Pompeian wall paintings⁶ and the 17th century painting *Adoration of the Magi* by Rubens.⁷ Although it is known that a combination of light, chlorine, and humidity influences the blackening, detailed knowledge on the exact conditions and the blackening capacity of other environmental compounds is lacking.

Thus, to counteract future degradation of both historic and modern pigments, insight into the chemical reactions that cause the degradation is essential for an appropriate conservation and preservation of valuable and irreplaceable paintings.

Studies on pigment degradation mainly focus on chemical analyses of historical paint samples using specialized techniques such as scanning electron microscopy (SEM), μ -X-ray diffraction (XRD), and X-ray absorption near-edge structure (XANES) analysis (e.g., refs 2, 4, 6, 8, and 9). Such investigations are complemented with monitoring studies of

Received: June 24, 2014

Accepted: August 27, 2014



74 model samples aged under specific conditions (e.g., refs 7 and
75 10–12). Although aging experiments often result in indis-
76 pensable information on the degradation process, these are
77 usually time-consuming: model samples for the complete
78 painter's palette need to be exposed to degrading agents such as
79 light, moisture, and gases for days up to months to mimic the
80 natural degradation during decades to centuries. However,
81 during such a time period, the single chemical transformations
82 such as the oxidation of a pigment is accompanied by other
83 unwanted slower transformations, for example, the sulfates
84 formed in situ from sulfidic pigments may dissolve in small
85 volumes of moisture present in the paint, migrating to the
86 surface and precipitating there together with any present
87 counterion.

88 To reduce the time needed to extract information on the
89 (photo)degradation of pigments, an alternative approach is
90 proposed, on the basis of electrochemical methods of detection.
91 In the heritage sector, the use of electrochemical methods is
92 already well-established in the branch of metal conservation and
93 restoration, and is applied for cleaning, stabilization, and
94 consolidation.^{13,14} Moreover, metal coupons or thin metal
95 sensors are used in the evaluation and monitoring of
96 environmental corrosivity, relating the formed corrosion layer
97 with the atmospheric conditions by using electrochemical
98 methods.^{15,16} In the past decade, electrochemistry has also been
99 introduced in the analysis, mainly identification, of other
100 heritage materials such as pigments and dyes^{17–20} and ceramic
101 materials.²¹ However, electrochemical methods did not yet find
102 their general use in the study of pigment degradation processes.
103 Apart from studying degradation products,⁵ a new electro-
104 chemical approach is developed for the real-time monitoring of
105 pigment degradation processes and the prediction of (environ-
106 mental) harmful conditions. The general concept consists of
107 depositing the pigment of interest on the surface of a graphite
108 electrode, mounting it in a three-electrode cell and monitoring
109 the degradation processes electrochemically. In the cell,
110 environmental conditions are mimicked by irradiating the
111 electrode with light of different wavelengths and intensity, while
112 exposing the pigment to an electrolyte compound present in
113 the atmosphere (e.g., an organic acid and water-soluble salts
114 present in airborne particles). By application of an appropriate
115 electrochemical method such as amperometry or linear sweep
116 voltammetry, details on the degradation process can be
117 gathered in a fast way by providing information on the changes
118 in photocurrent intensity or in the oxidation state of the metal
119 ions present. Effects of environmental parameters (light, air
120 aggressiveness, etc.) on the redox properties of the pigments
121 are not yet described in the literature. This work discusses how
122 the sensitivity toward such parameters can be estimated for
123 sulfide semiconductor pigments (e.g., orpiment (As_2S_3),
124 vermilion/cinnabar ($\alpha\text{-HgS}$), mosaic gold (SnS_2), and
125 cadmium yellow (CdS)). Experimental results for CdS and $\alpha\text{-HgS}$
126 are discussed, with main focus on the influence of
127 wavelength on the degradation process. In the future, the
128 approach could be extended with more advanced techniques
129 such as simultaneous (synchrotron-based) XRD, X-ray
130 absorption spectroscopy (XAS), or XANES analyses. Such
131 techniques help in the better understanding of the degradation
132 reactions, and the characterization of (insoluble) degradation
133 products in situ by using a special cell. Synchrotron
134 spectroelectrochemistry has already been described for the
135 corrosion monitoring of metal-based heritage objects.^{22–24}

EXPERIMENTAL SECTION

136

Graphite working electrodes ($\varnothing = 3 \text{ mm}$) were pretreated by
mechanical polishing with a P400 SiC paper to obtain a rough
surface. To remove any adherent SiC particles, the electrodes
were rinsed with deionized water and ethanol in an ultrasonic
bath for 15 s each. Subsequently, a 1 μL drop of either an
isopropanol– CdS suspension (0.05 g of CdS in 1 mL of
isopropanol) or an ethanol– HgS suspension (0.05 g of $\alpha\text{-HgS}$
in 1 mL of ethanol) was deposited onto the electrode surface
using a micropipette, relying on the VMP principle
(voltammetry of microparticles).^{13,25} The choice of solvent is
related to the most stable suspension of pigment grains in
solution. After solvent evaporation, a thin layer of the respective
pigment is left at the electrode surface. The modified electrodes
are denoted as ClCdS and $\text{Cl}\alpha\text{-HgS}$. A silver–silver chloride
(Ag|AgCl) electrode and a platinum (Pt) electrode were used
as the reference and counter electrode, respectively. The
electrodes were mounted in an open container, with the
pigment-modified side of the working electrode oriented
upward, enabling pigment irradiation using 30 mW lasers of
405 nm (blue), 532 nm (green), and 650 nm (red) pointing
downward (Figure 1). The Ag|AgCl reference electrode was

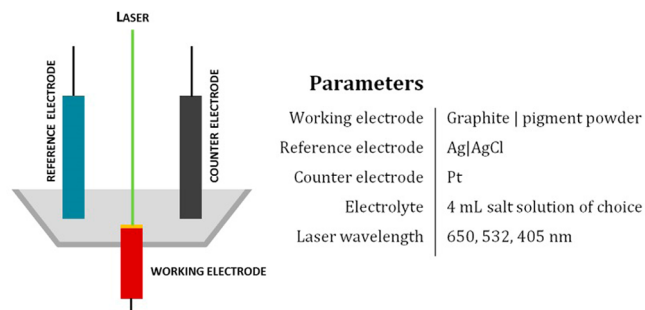


Figure 1. Electrochemical setup of a pigment-modified electrode with irradiation possibility.

protected from light illumination by covering it with aluminum
foil. The open container was filled with 4 mL of an electrolyte
of choice, providing approximately 0.5 cm of solution layer
above the electrode. To be sure that the laser beam was not
obstructed or significantly absorbed by the electrolyte, the
absorbance of the different electrolyte solutions was controlled
by UV–vis spectrophotometry (Cary 100 Dual Beam, Agilent
Technologies). Electrochemical experiments were performed
with an Autolab PGSTAT101 potentiostat (Metrohm, The
Netherlands) controlled by NOVA 1.10 software.

The experiments in the electrochemical cell were carried out
in two modes: (1) passive mode for long-term light irradiation
(up to 60 min), where the open circuit potential was measured
without applying any potential or current, and (2) active mode
in which amperometry at a constant potential was used when
short-term irradiation (few seconds) was applied to record the
photocurrent. This current was used to characterize the
pigment layer. Electrodes with freshly deposited pigments
showed noticeable well-detectable photocurrents while a bare
graphite electrode showed no photocurrents.

Absorption spectra of CdS and $\alpha\text{-HgS}$ were measured with
diffuse reflectance UV–vis spectrophotometry (DR–UV–vis)
(Evolution 500 UV–vis double-beam spectrophotometer with
RSA-UC-40 DR-UV integrated sphere, Thermo Electron
Corporation, Waltham, MA). The pigment powders were

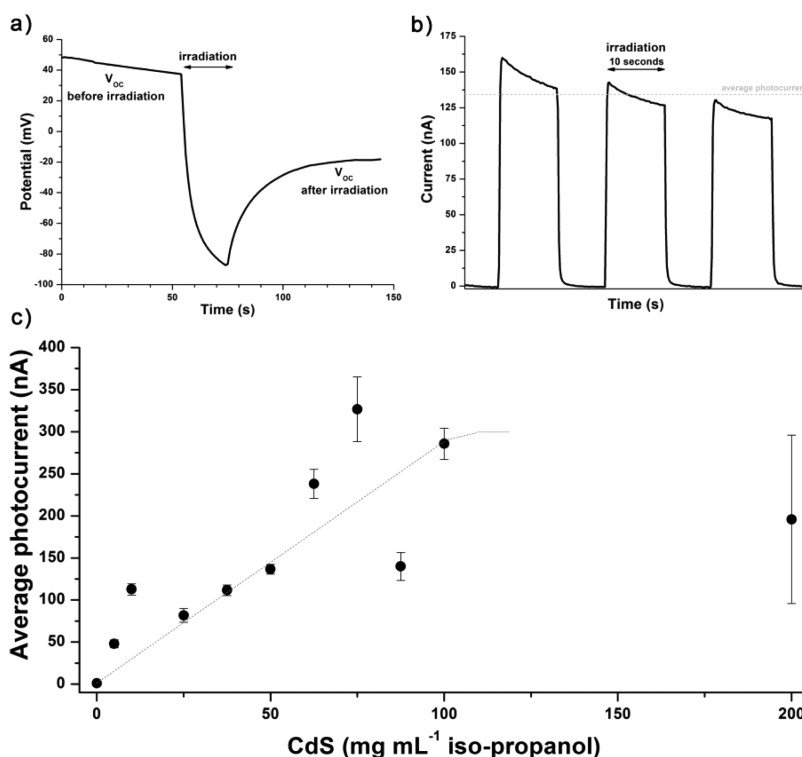
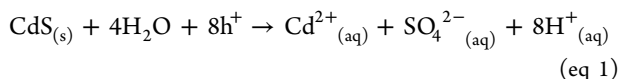


Figure 2. ClCdS electrode in 0.001 M NaCl, irradiation with green laser light (532 nm). (a) Open circuit potential (V_{OC}) before, during, and after illumination, (b) measured (photo)current in the dark and under illumination conditions, and (c) average CdS photocurrent vs CdS concentration in isopropanol suspension (error bars indicate the standard deviation).

183 mixed and crushed with KBr dried at 200 °C (0.02 g of CdS in
184 0.98 g of KBr and 0.015 g of HgS in 0.985 g of KBr). The
185 mixtures were homogeneous and positioned in the DR-UV-
186 vis cell for measuring in the 250–800 nm range.

187 ■ RESULTS AND DISCUSSION

188 **Cadmium Yellow.** CdS is a semiconductor with a band gap
189 energy (E_g) of ~2.4 eV. Upon illumination with supra band gap
190 light, electrons are excited from the valence band into the
191 conduction band. In an electrochemical cell, this results in a
192 potential drop of the working electrode and a rise of
193 “photocurrent” that originates from the ejection of excited
194 electrons from the CdS and the activation of oxidation
195 processes at the CdS working electrode (e.g., oxidation of
196 sulfide to sulfate). This is a typical behavior of an n-type
197 semiconductor.^{26,27} In the case of CdS in the presence of water
198 and oxygen, S^{2-} can be oxidized up to SO_4^{2-} , while Cd^{2+} is
199 formed (eq eq 1).²⁸ Water and oxygen may function as electron
200 acceptor.



202 In a first experiment, the relationship between the amount of
203 CdS deposited on the electrode and the photocurrent was
204 studied by preparing different ratios of CdS–isopropanol
205 suspensions. First, the open circuit potential V_{OC} was
206 determined for each ClCdS electrode, using a 0.001 M NaCl
207 solution as electrolyte. The potential between electrode surface
208 and solution was clearly different for the period before, during,
209 and after illumination. As shown in Figure 2a, illumination
210 causes a sudden decrease in V_{OC} . Since thermodynamically the
211 potential is directly proportional to Gibbs free energy ($\Delta G^0 =$

212 $-nF(E_{\text{reduction}} + E_{\text{oxidation}})$),²⁹ this indicates that CdS becomes
213 more prone to chemical oxidation reactions upon illumination
214 due to the change in Fermi energy (E_F) and band bending.^{30,31}
215 After irradiation, V_{OC} slowly stabilizes. This V_{OC} was
216 subsequently taken as the potential for amperometric measure-
217 ments and allows the electrode to be near the equilibrium in
218 the dark. In this way, the background was not influenced by any
219 overpotential and resembled most to a “natural” environment.
220 Because of the formation of degradation products and a change
221 in the initial state of the surface, the V_{OC} in the dark slightly
222 changes over the experiment.

223 During the amperometric measurement, four alternating
224 cycles of darkness (~10 s) and illumination (10 s) with a green
225 laser (532 nm) were used (Figure 2b). The photocurrent was
226 calculated as the average of the last three illumination cycles,
227 with a correction for the (mostly negligible) dark current. The
228 small decrease in photocurrent observed during each cycle is
229 due to the oxidation of the CdS pigments grains, dissolving
230 Cd^{2+} and SO_4^{2-} . For every concentration ratio, the experiment
231 was repeated for at least three different electrodes.

232 A clear trend is observed: the more CdS is present, the
233 higher the photocurrent (Figure 2c). Since higher amounts of
234 CdS result in a lower fraction of pigment particles to be in
235 direct contact with the graphite electrode, while a thicker
236 pigment layer partially blocks illumination of the CdS in
237 contact with the electrode, the linearity of the response is
238 limited. Therefore, with very high amounts of CdS (>200 mg
239 mL⁻¹ isopropanol), the photocurrent does not increase
240 anymore and larger deviations appear.

241 The ClCdS electrode preparation procedure does not allow
242 for perfect control of the amount and distribution of CdS on
243 the electrode. A clearly better reproducibility is obtained at
244 lower CdS concentrations. Therefore, subsequent experiments 244

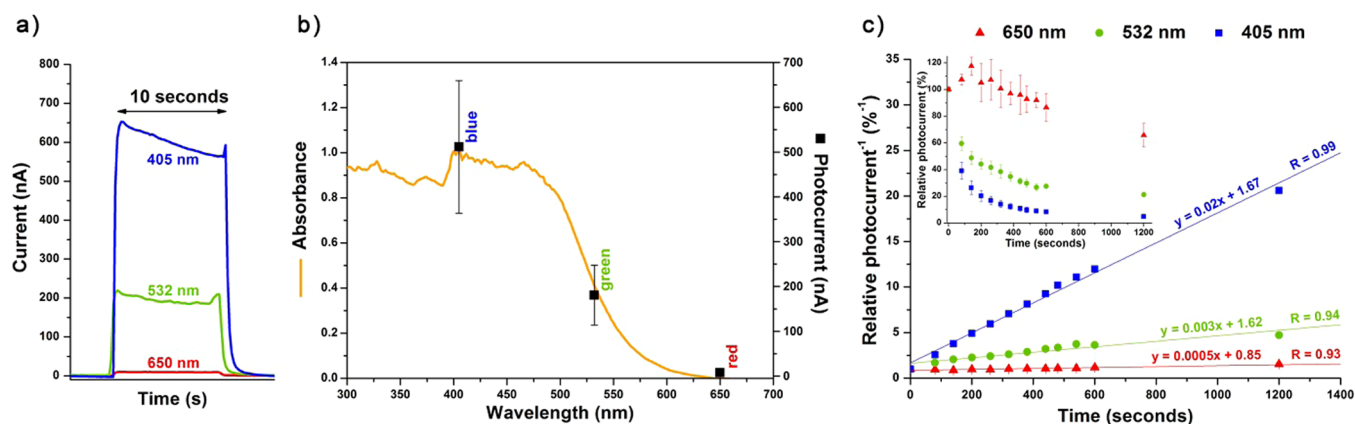


Figure 3. (a) ClCdS electrode, subsequently illuminated with 650, 532, and 405 nm wavelengths. (b) CdS absorption spectrum with photocurrents for irradiation with 650, 532, and 405 nm wavelengths. (c) Degradation kinetics of CdS in a 0.001 M NaCl solution and irradiation (405, 532, and 650 nm wavelengths).

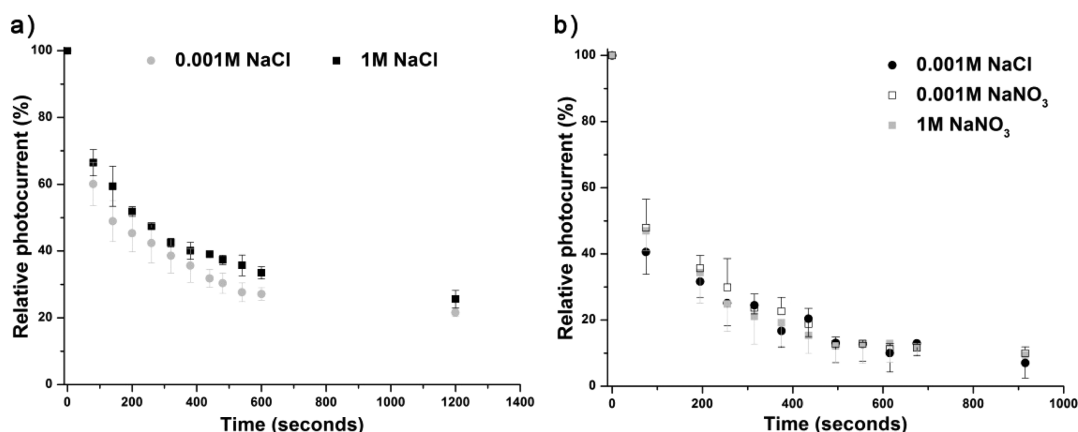


Figure 4. (a) Degradation kinetics of CdS in 0.001 and 1 M NaCl solution (irradiation with 532 nm wavelength). (b) Degradation kinetics of CdS in 0.001 M NaCl, and 0.001 and 1 M NaNO₃ solution (irradiation with 405 nm wavelength).

were performed with a 50 mg mL⁻¹ isopropanol suspension of CdS.

Figure 3a shows the photocurrent for a single ClCdS electrode, subsequently illuminated with red, green, and blue lasers. For each wavelength, three illumination cycles of 10 s were applied. Figure 3a only shows one illumination cycle. The experiment was repeated for five different electrodes. Although illumination of each electrode was limited to 30 s per wavelength, the sequence of red, green, and blue laser illumination was varied to eliminate the influence of previous degradation. However, no significant difference was observed. For each wavelength, the average photocurrent of the five electrodes was subsequently plotted onto the absorption spectrum of the CdS powder (Figure 3b). The pseudoabsorbance spectrum shows a typical shape for a semiconductor material, exhibiting an absorption edge near 564 nm, corresponding to a band gap of 2.2 eV. Since the red laser has an energy below the CdS absorbance band ($h\nu < E_g$), only a very small photocurrent (~ 5 nA) is observed. The wavelength of the green laser is situated in the middle of the absorption edge, inducing a partial excitation of the CdS. The blue laser light, in contrast, is fully absorbed, generating the highest photocurrent.

Since the photocurrent is dependent on the amount of CdS on the electrode (Figure 2c), a gradual decrease in photocurrent is expected when the CdS pigment becomes more

degraded by photoinduced oxidation. Indeed, as the expected oxidation product CdSO₄·xH₂O is water-soluble and does not possess semiconductor properties, it will not contribute to the measured photocurrent. In this manner, the setup provides the possibility to electrochemically monitor the degradation of CdS versus time under different conditions. As an example, the degradation kinetics of CdS were measured during illumination with red, green, and blue lasers in a 0.001 M NaCl electrolyte. Analogous to the previous experiment, the stabilized V_{OC} was first determined, and subsequently used as the fixed potential during amperometric measurements (i.e., the active mode). Then the electrodes were illuminated for a certain time interval without any electrochemical intervention (i.e., in passive mode). Afterward, the next amperometric measurement was performed. This sequence was continued up to 20 min light irradiation. For each wavelength, the experiment was repeated for three different electrodes. For both the green and blue laser light, a clear solubilization of the CdS occurred, visible by a disappearance of the bright colored powder in the area where the laser irradiated the electrode. Figure 3c represents the degradation kinetics at the three wavelengths as the relative photocurrent (inset) and as the inverse of the relative photocurrent. For both the green and blue laser a clear photocurrent decay (hyperbolic trend) is followed, strongly suggesting a second-order decay reaction. This could indicate that the degradation involves more complicated reactions. Also

pigment grain size could be a factor of influence. More research is needed to clarify this trend. The photocurrent decay depends on the excitation wavelength used: after 20 min of illumination, a decay of $79 \pm 1\%$ (green laser) and $95 \pm 1\%$ (blue laser) is observed. The large error observed for the red laser is related to the very low photocurrents measured, and should be considered with caution. Nevertheless, a small decrease in photocurrent is observed, corresponding to a decay of $\sim 34 \pm 9\%$ after 20 min of irradiation. This is attributed to defect states in the CdS structure, creating energy levels in the band gap, and assisting in the light absorption process (trap-to-band transitions). The limited photocurrent (Figure 3a) indicates that this process is not efficient and only a small amount of CdS is oxidized compared to the green and blue laser.

Since it is generally advised not to use highly diluted electrolytes to avoid effects of increased solution resistance, ion migration, and unclear surface charge at the electrode–solution interface,³² the irradiation experiment with the green laser was repeated for a 1 M NaCl electrolyte (Figure 4a). An upward shift of 3% relative photocurrent was observed for the 1 M NaCl compared to the 0.001 M NaCl, lying within the experimental error. The same experiment with 0.001 M NaCl, 0.001 M NaNO₃, and 1 M NaNO₃ (blue laser irradiation) also results in similar degradation kinetics (Figure 4b). Therefore, the presence or absence of these salts does not significantly influence the degradation of the CdS powder.

With adjustment of the experimental setup, different light sources and hazardous environmental compounds could now be tested on their damaging effects toward CdS. Light source such as LED, halogen, and glass fibers with varying temperature color could be evaluated for their photo-oxidizing capacity. In conservation practice, light sensitivity of materials is commonly expressed in illuminance (lux). Also, the influence of this parameter could be easily evaluated by varying the amount of light that strikes the electrode per surface area.

Vermilion. α -HgS is an n-type semiconductor with $E_g \sim 2$ eV. However, its degradation appears more complex compared to that of CdS. Figure 5 shows the photocurrent versus time

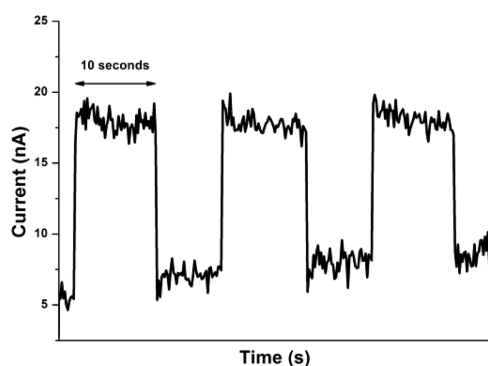


Figure 5. Amperometry of a Cl α -HgS electrode in 0.001 M NaCl with alternating dark-illumination cycles (green laser).

during alternating cycles of darkness and illumination with 532 nm light in 0.001 M NaCl. The potential used is determined in a manner analogous to that for CdS. The positive photocurrent suggests an oxidation process as expected for an n-type semiconductor. Since the photocurrent is remarkably lower compared to that for CdS, fewer oxidation products are formed. For the real-time monitoring of the degradation process, amperometric measurements were performed during continu-

ous illumination, following up the change in photocurrent. The experimental setup was employed to evaluate the effect of light with different wavelengths on the degradation of α -HgS. Cl α -HgS electrodes were monitored during a 1 h illumination in 1 M NaCl (Figure 6a). Under the conditions used, after around 6 and 12 min of illumination with the blue and green laser, respectively, the photocurrent starts to increase instead of decreasing as was the case for CdS (Figure 3c). Afterward, the current decreased again, but even after 60 min of illumination, it is still significantly higher compared to the initial current recorded. For the red laser, the current increase is negligible.

A photocurrent increase for α -HgS has already been observed by Davidson and Willsher³³ and corresponds to a slight blackening of the electrode, visible with the naked eye. Also, in the experiments performed in the current study, the photocurrent increase is related to the blackening of α -HgS. Previous research assigned this discoloration to the formation of Hg⁰.⁵ To confirm the presence or absence of Hg⁰ after the amperometric monitoring, additional control with linear sweep voltammetry from -200 to 75 mV was performed, using 0.1 M NaOH as electrolyte. The Hg⁰/Hg²⁺ oxidation peak is situated around -50 mV, whereas α -HgS does not show any redox transformation in the applied potential range.⁵ The voltammetric control measurement confirms the formation of Hg⁰ for the blue and green laser, while after red light illumination, no Hg⁰ is formed. Since red light does not have enough energy to excite electrons from the valence band into the conduction band of α -HgS, the absence of Hg⁰ with red light illustrates that electron excitation is mandatory to induce blackening of α -HgS.

The photocurrent increase may be attributed to a catalytic effect of the (discontinuous) film of metallic mercury (nano)particles that is formed in situ,⁵ changing the energetics of the electron-transfer process at the semiconductor surface.³¹ If metallic mercury is formed at the surface of the α -HgS particles, a superior electric contact between semiconductor and graphite electrode is formed. Hg⁰ can facilitate the transport of excited electrons toward adsorbed Hg²⁺ species, inducing a faster formation of Hg⁰. In addition, Hg⁰ can cause a larger fraction of the pigment to be in contact with the electrode due to the increase of the conductive surface, possibly improving the kinetics of the sulfide oxidation. The faster increase in photocurrent for the blue laser suggests a faster Hg⁰ production. After some period of time, the photocurrent starts to drop. This can have different causes such as a decreasing amount of α -HgS that can participate in the oxidation reaction, a preferential oxidation of Hg⁰ compared to the semiconductor, and/or the formation of a continuous Hg⁰ film which partly blocks the amount of light that can be absorbed by the underlying α -HgS.³¹

The harmful effect of chlorides on the blackening of α -HgS is a well-known phenomenon.^{1,19,5,26} The setup was also used to identify the blackening capacity of other environmental compounds by using them as the electrolyte. In this way, additional experiments with green laser illumination proved the deleterious effects of organic acids such as formic and acetic acid and ammonium-rich compounds such as NH₄NO₃ and (NH₄)₂SO₄, both present in airborne particulate matter (Figure 7). However, the degradation kinetics are slower compared to when NaCl is present: the increase in photocurrent appears later and/or shows a less steep increase. Other compounds such as NaNO₃ and Na₂SO₄ showed a negligible increase in photocurrent within the tested time span. Analogous to the experiment shown in Figure 6b, linear sweep voltammetry was

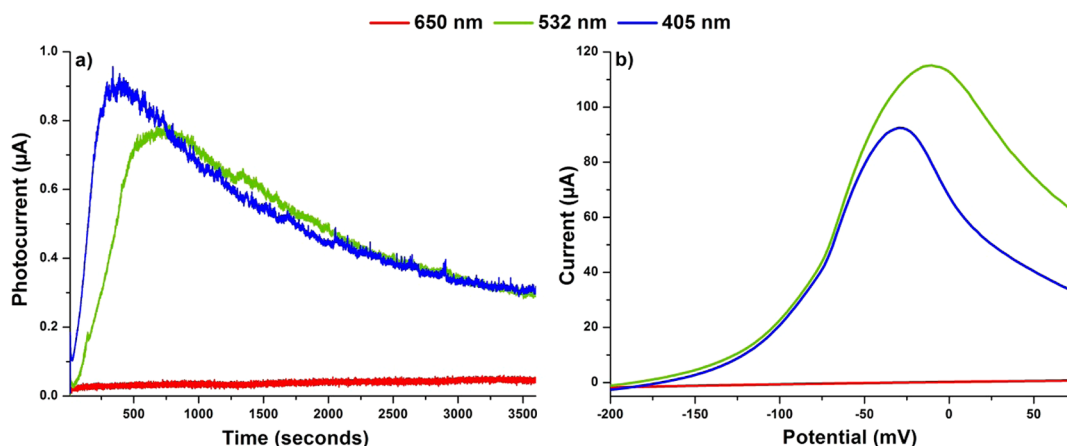


Figure 6. Comparison of three different wavelengths on the degradation capacity of α -HgS. (a) Chronoamperometric measurement during 1 h illumination in 1 M NaCl, illustrating the catalyzing effect of the degradation product. (b) Linear sweep voltammograms in 0.1 M NaOH after 1 h of illumination, confirming the in situ formation of Hg^0 in case of the green and blue lasers, and the absence of Hg^0 with the red laser.

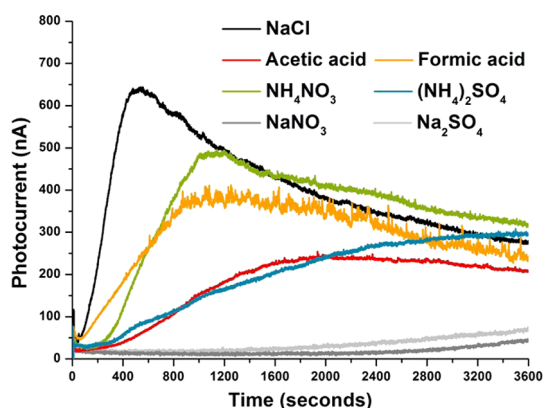


Figure 7. Comparison of different environmental compounds on the degradation capacity of α -HgS. Chronoamperometric measurements during 1 h illumination (green laser) in 1 M solutions.

a risk assessment though, in the current study, the pigments were used in their pure form, without taking into account combinations of materials typically present in paintings (e.g., binding medium and mixtures with other (inorganic) pigments). Also, the influence of the semiconductor grain size toward their environmental stability could be studied. Such more complex conditions are the obvious step in understanding the degradation phenomena in real paintings. However, they present challenges. To study pigment mixtures and grain sizes, it is necessary to exactly control the amount of semiconductor deposited onto the electrode, and to ensure a homogeneous dispersion. Binding media such as oil (partially) block the contact between the pigment and the graphite electrode. However, electrochemical experiments require a contact interface between the electrode material and the pigment. This hinders mimicking a more realistic paint situation in which most pigment grains are initially well encapsulated in the binding medium. At this moment, experiments are ongoing to overcome these challenges.

For both CdS and α -HgS, illumination with supra band gap light induces an oxidative degradation, though CdS appeared more prone to oxidation compared to α -HgS, based on its remarkable higher photocurrent. Where the electrolyte composition is of less importance for CdS, it has a major influence for α -HgS: certain compounds such as chlorides induce secondary reactions, forming Hg^0 . This alteration product induces an increase in photocurrent, catalyzing the degradation process. Apart from semiconductor pigments, the electrochemical approach could also be used for other pigments exhibiting redox reactions as part of their degradation behavior (e.g., chrome yellow).

The electrochemical experiments are presented as an alternative to classical time-consuming accelerated aging experiments. However, not all natural aging phenomena can be reproduced in the electrochemical experiments. A main reason is the liquid environment in the electrochemical cell. Processes such as dissolution–recrystallization cycles of soluble degradation products (e.g., cadmium sulfates) due to variations in ambient relative humidity do not occur in the electrochemical cell. Also, secondary reactions with pigment degradation products and their environment can be hindered by the liquid environment. It is for example hypothesized that Hg^0 , the black degradation product of α -HgS, further reacts

performed after the chronoamperometric measurement to confirm the formation of Hg^0 . A $\text{Hg}^0/\text{Hg}^{2+}$ peak appeared for acetic and formic acid, and NH_4NO_3 and $(\text{NH}_4)_2\text{SO}_4$. No Hg^0 was detected for NaNO_3 and Na_2SO_4 , both showing a negligible photocurrent increase. Therefore, these compounds can be considered as harmless regarding α -HgS blackening.

CONCLUSION

The proposed electrochemical method for a fast and real time monitoring of pigment degradation gives interesting and promising results for semiconductor pigments such as CdS and α -HgS. By using amperometry at the open circuit potential (V_{OC}), the degradation can be followed up and evaluated under various conditions. The conditions can be varied in (1) the type of sample (i.e., pigment), (2) the type of irradiation, and (3) the type of electrolyte.

Different light sources can be tested on their damaging effects toward semiconductor pigments. The experimental setup can easily be adjusted, taking into account the type of light, illuminance, and color temperature. In addition, the influence of different types of hazardous environmental compounds can be evaluated, provided that they can serve as (aqueous) electrolyte (e.g., organic acids and salts occurring in airborne particles). Results of such experiments help in the identification of environmental hazards, for example, to draw up

with Cl^- to form HgCl_2 or Hg_2Cl_2 .^{5,9} Such reactions are (partially) hindered in large volumes of water in which Cl^- easily dissolves. Despite this disadvantage, the electrochemical monitoring experiments are very useful to speed up the degradation reactions, dissociate different steps in complex degradation phenomena, and study degradation kinetics in various environments. The proposed methodology could be applied to study all redox-active substances that react under a physical stimulus such as light, or interact with a chemical reagent.

AUTHOR INFORMATION

Corresponding Author

*E-mail: Karolien.DeWael@uantwerpen.be.

Notes

The authors declare no competing financial interest.

ACKNOWLEDGMENTS

The authors thank Vera Meynen and Monika Kus of the University of Antwerp, Laboratory of Adsorption and Catalysis (LADCA), for the provision and help with the DR–UV–vis.

REFERENCES

- (1) Fiedler, I.; Bayard, M. A. In *Artists' Pigments. A Handbook of their History and Characteristics*; Feller, R. L., Ed.; Cambridge University Press: Cambridge, 1986; pp 65–108.
- (2) Van der Snickt, G.; Dik, J.; Cotte, M.; Janssens, K.; Jaroszewicz, J.; De Nolf, W.; Groenewegen, J.; Van der Loeff, L. *Anal. Chem.* **2009**, *81*, 2600–2610.
- (3) Mass, J. L.; Opila, R.; Buckley, B.; Cotte, M.; Church, J.; Mehta, A. *Appl. Phys. A: Mater. Sci. Process.* **2013**, *111*, 59–68.
- (4) Van der Snickt, G.; Janssens, K.; Dik, J.; De Nolf, W.; Vanmeert, F.; Jaroszewicz, J.; Cotte, M.; Falkenberg, G.; Van der Loeff, L. *Anal. Chem.* **2012**, *25*, 25.
- (5) Anaf, W.; Janssens, K.; De Wael, K. *Angew. Chem., Int. Ed.* **2013**, *52*, 12568–12571.
- (6) Cotte, M.; Susini, J.; Metrich, N.; Moscato, A.; Gratziau, C.; Bertagnini, A.; Pagano, M. *Anal. Chem.* **2006**, *78*, 7484–7492.
- (7) Radepon, M.; de Nolf, W.; Janssens, K.; Van der Snickt, G.; Coquinot, Y.; Klaassen, L.; Cotte, M. *J. Anal. At. Spectrom.* **2011**, *26*, 959–968.
- (8) Cotte, M.; Susini, J.; Sole, V. A.; Taniguchi, Y.; Chillida, J.; Checroun, E.; Walter, P. *J. Anal. At. Spectrom.* **2008**, *23*, 820–828.
- (9) Keune, K.; Boon, J. *J. Anal. Chem.* **2005**, *77*, 4742–4750.
- (10) Monico, L.; Van der Snickt, G.; Janssens, K.; De Nolf, W.; Miliani, C.; Verbeeck, J.; Tian, H.; Tan, H.; Dik, J.; Radepon, M.; Cotte, M. *Anal. Chem.* **2011**, *83*, 1214–1223.
- (11) Monico, L.; Van der Snickt, G.; Janssens, K.; De Nolf, W.; Miliani, C.; Dik, J.; Radepon, M.; Hendriks, E.; Geldof, M.; Cotte, M. *Anal. Chem.* **2011**, *83*, 1224–1231.
- (12) Leone, B.; Burnstock, A.; Jones, C.; Hallebeek, P.; Boon, J. J.; Keune, K. In *14th Triennial Meeting, The Hague, 12–16 September 2005: Preprints (ICOM Committee for Conservation)*; Verger, L., Ed.; Earthscan Ltd.: Oxford, 2005; pp 803–813.
- (13) Doménech-Carbó, A.; Doménech-Carbó, M. T.; Costa, V. *Electrochemical Methods in Archaeometry, Conservation and Restoration*; Springer: Berlin, 2009.
- (14) Barrio, J.; Chamón, J.; Pardo, A. I.; Arroyo, M. *J. Solid State Electrochem.* **2009**, *13*, 1767–1776.
- (15) Costa, V.; Texier, A.; de Reyer, D. Impact of Environmental Conditions on Metallic Artifacts from the Treasure Rooms of Reims Cathedral. In *Heritage, Weathering and Conservation*; Fort, R.; Alvarez de Buergo, M.; Gomez Heras, M.; Vazquez-Clavo, C., Eds.; Taylor & Francis Group: London, 2006; pp 453–456.
- (16) Prosek, T.; Kouril, M.; Dubus, M.; Taube, M.; Hubert, V.; Scheffel, B.; Degres, Y.; Jouannic, M.; Thierry, D. *Stud. Conserv.* **2013**, *58*, 117–128.
- (17) Grygar, T.; Bezdicka, P.; Hradil, D.; Doménech-Carbo, A.; Marken, F.; Pikna, L.; Cepria, G. *Analyst* **2002**, *127*, 1100–1107.
- (18) Doménech-Carbó, A.; Doménech-Carbó, M. T.; Mas-Barbera, X. *Talanta* **2007**, *71*, 1569–1579.
- (19) Komorsky-Lovric, S.; Mirceski, V.; Scholz, F. *Mikrochim. Acta* **1999**, *132*, 67–77.
- (20) Doménech-Carbó, A.; Doménech-Carbó, M. T.; Calisti, M.; Maiolo, V. *Talanta* **2010**, *81*, 404–411.
- (21) Doménech-Carbó, A.; Doménech-Carbó, M. T.; Osete-Cortina, L.; Gimeno-Adelantado, J.; Bosch-Reig, F.; Mateo-Castro, R. *Talanta* **2002**, *56*, 161–174.
- (22) Adriaens, A.; Dowsett, M. *Acc. Chem. Res.* **2010**, *43*, 927–935.
- (23) Monnier, J.; Reguer, S.; Foy, E.; Testemale, D.; Mirambet, F.; Saheb, M.; Dillmann, P.; Guillot, I. *Corros. Sci.* **2014**, *78*, 293–303.
- (24) Leyssens, K.; Adriaens, A.; Dowsett, M. G.; Schotte, B.; Oloff, I.; Pantos, E.; Bell, A. M. T.; Thompson, S. P. *Electrochem. Commun.* **2005**, *7*, 1265–1270.
- (25) Scholz, F.; Gulaboski, R.; Schröder, U. *Electrochemistry of Immobilized Particles and Droplets*; Springer-Verlag: Berlin, 2005.
- (26) Zhang, Z.; Yuan, Y.; Fang, Y.; Liang, L.; Ding, H.; Shi, G.; Jin, L. *J. Electroanal. Chem.* **2007**, *610*, 179–185.
- (27) Davidson, R. S.; Willsher, C. J. *Nature* **1979**, *278*, 238–239.
- (28) Meissner, D.; Memming, R. *Ber. Bunsen-Ges. Phys. Chem.* **1985**, *89*, 121–124.
- (29) Gileadi, E. *Physical Electrochemistry. Fundamentals, Techniques and Applications*; Wiley-VCH Verlag GmbH & Co. KGaA: Weinheim, 2011.
- (30) Zhang, Z.; Yates, J. T., Jr. *Chem. Rev.* **2012**, *112*, 5520–5551.
- (31) Walter, M. G.; Warren, E. L.; McKone, J. R.; Boettcher, S. W.; Mi, Q.; Santori, E. A.; Lewis, N. S. *Chem. Rev.* **2010**, *110*, 6446–6473.
- (32) Gerischer, H. *Electrochim. Acta* **1990**, *35*, 1677–1699.
- (33) Davidson, R. S.; Willsher, C. J. *J. Chem. Soc., Faraday Trans.* **1980**, *76*, 2587–2603.